Endoplasmic Reticulum Chaperone GRP94 Subunit Assembly Is Regulated through a Defined Oligomerization Domain†

Pamela A. Wearsch and Christopher V. Nicchitta*

Department of Cell Biology, Duke University Medical Center, Durham, North Carolina 27710

Received August 16, 1996; Revised Manuscript Received November 1, 1996⊗

ABSTRACT: GRP94 is an abundant, resident glycoprotein of the mammalian endoplasmic reticulum lumen and member of the hsp90 family of molecular chaperones. To identify the structure/function relationships which define the molecular basis of GRP94 activity, we have performed a structural analysis of native GRP94 and identified a discrete domain, representing amino acids 676−719, which regulates dimerization and displays autonomous oligomerization activity. Velocity sedimentation and gel filtration chromatography were used to identify native GRP94 as a dimer with an extended, rod-like shape. Limited proteolysis resulted in the loss of approximately 16 kDa from the C-terminus and disassembly into monomers, implicating the C-terminus as the site of assembly. An assembly function for the C-terminal domain was established by analysis of the quaternary structure of C-terminal constructs synthesized either in vitro or through recombinant expression. In vitro translation was used to demonstrate that a C-terminal 20 kDa domain was both necessary and sufficient for dimerization. Structural studies of recombinant fusion protein constructs yielded identification of a 44 amino acid domain that displayed autonomous dimerization activity and conferred a highly elongated structure, characteristic of native GRP94, to the fusion protein. These data, combined with molecular dimensions obtained from rotary shadowing electron microscopy, provide a structural model of GRP94 and identify the molecular basis of GRP94 self-assembly.

The lumen of the endoplasmic reticulum (ER)[1] is highly enriched for proteins whose functions identify the ER as an organelle specializing in protein biosynthesis. Included are enzymes, such as protein disulfide isomerase (PDI), which catalyzes the formation of disulfide bonds, and molecular chaperones, such as BiP, which function in protein folding and assembly (Freedman et al., 1988; Flynn et al., 1989; Gething & Sambrook, 1992; Peterson et al., 1995). In addition to their role in protein folding and assembly, recent evidence indicates that ER chaperones function in protein translocation, particularly at late stages when the nascent chain has gained access to the ER lumen (Vogel et al., 1990; Nguyen et al., 1991; Sanders et al., 1992; Nicchitta & Blobel, 1993; Brodsky et al., 1995). Chaperones are also thought to play a central role in the ER quality control mechanism which functions to prevent the export of malfolded proteins into the secretory pathway (Fra & Sitia, 1993; Knittler et al., 1995).

The protein composition of the mammalian ER lumenal compartment is relatively simple, consisting predominately of five proteins: GRP94, BiP, ERp72, PDI, and calreticulin. BiP (GRP78), the hsp70 homolog of the ER, was first discovered through its association with immunoglobulin heavy chains (Munro & Pelham, 1986; Haas & Wabl, 1983). In yeast, BiP (Kar2p) is essential for viability (Rose et al., 1989; Normington et al., 1989) and has been shown to play a direct role in protein translocation (Vogel et al., 1990; Nguyen et al., 1991; Sanders et al., 1992; Brodsky et al., 1995). The finding that BiP binds to peptides, and in particular those which are hydrophobic in nature (Flynn et al., 1989, 1991; Blond-Elguindi et al., 1993a), has lead to the hypothesis that BiP regulates protein folding through suppression of aggregation and nonproductive interactions of exposed hydrophobic side chains (Pelham, 1986; Rothman, 1989; Gething & Sambrook, 1992). PDI, also essential for viability in yeast, is a member of the thioredoxin superfamily and catalyzes oxidation/reduction of disulfide bonds (Farquhar et al., 1991; Creighton et al., 1980). ERp72 is a member of the thioredoxin superfamily and functions in disulfide bond exchange (Mazzarella et al., 1990; Gunther et al., 1993). Calreticulin was identified as the major calcium binding protein of the endoplasmic reticulum (Macer & Koch, 1988). Recent experimental evidence indicates that calreticulin is a molecular chaperone and functions in a manner similar to calnexin, its ER transmembrane homolog, in the regulation of glycoprotein folding (Peterson et al., 1995; Helenius, 1994). GRP94 is a member of the hsp90 family of molecular chaperones (Sorger & Pelham, 1987; Mazzarella & Green, 1987) and has been described as the most abundant mammalian ER lumenal protein (Koch et al., 1986; Wearsch & Nicchitta, 1996). With regard to function, however, GRP94 is the least understood of the ER chaperones.

A chaperone activity for GRP94 has been proposed on the basis of two primary observations. Foremost, the expression of GRP94 is coordinately regulated with BiP and is increased by glucose starvation as well as experimental conditions that result in the lumenal accumulation of unfolded proteins (Lee, 1987; Kozutsumi et al., 1988; Lenny & Green,

† This work was supported by NIH Grant DK47897 (C.V.N.).

* To whom correspondence should be addressed. Phone: (919) 684-8948; Fax: (919) 684-5481; E-mail: chris_nicchitta@cellbio.duke.edu.

⊗ Abstract published in *Advance ACS Abstracts,* December 15, 1996.

[1] Abbreviations: BiP, binding protein; ER, endoplasmic reticulum; $f/f_{min,}$ frictional ratio; GRP, glucose regulated protein; hsp, heat shock protein; MBP, maltose binding protein; PBS, phosphate buffered saline; PDI, protein disulfide isomerase; R_s, Stokes radius; *s*, sedimentation coefficient.

S0006-2960(96)02068-5 CCC: $12.00

1991). Second, GRP94 has been found to associate with a limited number of substrates including immunoglobulins, MHC class II molecules, HSV-1 glycoprotein B, thyroglobulin, and collagen (Melnick et al., 1992; Schaiff et al., 1992; Navarro et al., 1991; Kuznetsov et al., 1994; Ferreira et al., 1994). Studies of the kinetics of chaperone−nascent chain interactions indicate that GRP94 can associate with substrates subsequent to BiP, indicating that GRP94 may recognize relatively mature structural elements of newly assembling proteins (Melnick et al., 1994).

Peptide binding is an inherent property of many molecular chaperones and has been well characterized for BiP and members of the hsp70 family (Flynn, 1991; Blond-Elguindi et al., 1993a; Fourie et al., 1994; Gragerov & Gottesman, 1994). Evidence that GRP94 is also a peptide binding protein has recently been obtained through identification of GRP94 as a tumor-rejection antigen of methylcholanthrene-induced murine sarcomas (Srivastava et al., 1986). Srivastava et al. (1986) demonstrated that vaccination of mice with sarcoma-derived GRP94 results in a substantial immune response to subsequent challenges with the parent tumor cells. This activity was attributed to a tightly bound, tumor-derived, peptide fraction (Li & Srivastava, 1993). Further experimental evidence for a peptide binding function for GRP94 has been provided in studies demonstrating that immunization of mice with GRP94 purified from β-galactosidase overexpressing cell lines induced β-galactosidase-specific cytotoxic T-lymphocytes (CTL's) (Arnold et al., 1995). In a related study, macrophages pulsed with GRP94 purified from vesicular stomatitus virus (VSV) infected cells were targets for lysis by VSV-specific CTL's (Suto & Srivastava, 1995). The induction of a CTL response requires the transfer of GRP94-derived peptides onto MHC class I molecules, and thus GRP94 is capable of binding peptides of as yet undetermined size and sequence characteristics. To date, the functional relationship between the peptide binding and chaperone activity of GRP94 is unclear.

In light of the abundance and ubiquitous distribution of GRP94 in mammalian cells, as well as the paucity of insight concerning its cellular function, we have initiated a series of studies on the structure/function relationships which define the molecular mechanism of GRP94 action. In this paper, we present a structural analysis of native GRP94, identified as an obligatory dimer with an extended, rod-like structure. A discrete domain, corresponding to amino acid residues 676−719, has been identified which regulates dimeric assembly and displays autonomous and transferable oligomerization activity. These findings have been incorporated into a structural model of GRP94 and provide a framework for future studies on its chaperone activity.

EXPERIMENTAL PROCEDURES

Reagents. Zwittergent 3-12 was purchased from Calbiochem (La Jolla, CA). The pMAL-c2 vector, amylose resin, and factor Xa protease were obtained from New England Biolabs (Beverly, MA). Nucleotides as well as protein standards for gel filtration and velocity sedimentation were obtained from Pharmacia Biotech Inc. (Piscataway, NJ).

Antibodies. A polyclonal antibody generated against a peptide corresponding to the N-terminal 14 amino acids of canine GRP94 was a generous gift of Dr. Steve Cala (Wayne State University, Detroit, MI). Rabbit polyclonal antisera (DU-32) generated against a domain corresponding to the C-terminal 44 amino acids of the canine GRP94 sequence was prepared according to the protocol of Harlowe and Lane (1988). The sequence encoding the C-terminal 44 amino acids from the canine GRP94 cDNA (94C) was cloned as a fusion with GST (glutathione *S*-transferase) in the pGEX-2T vector (Pharmacia Biotech Inc., Piscataway, NJ). GST-94C fusion protein was expressed in *Escherichia coli* strain BL21 and purified by affinity chromatography according to the manufacturer's instructions. Primary injections (0.5 mg) of GST-94C were performed in Freund's complete adjuvant, and secondary injections (0.2 mg) were in Freund's incomplete adjuvant.

Purification of Porcine GRP94. GRP94 was purified from porcine pancreatic rough microsomes as described in Wearsch and Nicchitta (1996). Rough microsomes were made following the protocol of Walter and Blobel (1983).

Gel Filtration Chromatography. A TSK-GEL G3000 SW analytical gel filtration column (Tosohaus, Montgomeryville, PA) was equilibrated in either PBS (phosphate buffered saline) or buffer A (110 mM KOAc, 25 mM K-Hepes, pH 7.2, 20 mM NaCl, 1 mM $Mg(OAc)_2$, 0.1 mM $CaCl_2$). Samples in a volume of 125 μL were injected onto the column at a flow rate of 0.6 mL/min. Fractions of 0.5 mL were collected and analyzed by SDS−PAGE. The Stokes radius (R_s) for each sample was determined by comparison with standards (thyroglobulin, R_s = 8.5 nm, 660 kDa; apoferritin, R_s = 6.1 nm, 440 kDa; aldolase, R_s = 4.8 nm, 160 kDa; BSA, R_s = 3.5 nm, 66 kDa; ovalbumin, R_s = 3.1 nm, 43 kDa). Where indicated, GRP94 was incubated with 4 mM Zwittergent 3-12 for 45 min at RT in 125 μL of buffer A or 1× PBS prior to analysis.

Velocity Sedimentation. For the determination of sedimentation coefficients (*s*), samples were analyzed on sucrose gradients in parallel with known standards. Native GRP94, elastase-digested GRP94, and in vitro synthesized GRP94-ΔC (see Construct Preparation) were analyzed on gradients of 15−30% sucrose supplemented with buffer A. In vitro synthesized GRP94-Cexp translation products and GRP94−MBP fusion proteins were analyzed on 10−25% sucrose gradients supplemented with PBS. Gradients of 11.5 mL were prepared and harvested with an Auto Densi-Flow IIc (Buchler Instruments, Lenexa, KS). Samples in a volume of 200 μL were loaded onto gradients and centrifuged in the Beckman SW41 rotor at 40 000 rpm for 20 h at RT. Catalase (11.3 S), yeast alcohol dehydrogenase (7.4 S), BSA (4.3 S), ovalbumin (3.5 S), and chymotrypsinogen A (2.6 S) were employed as standards. Fractions of 0.5 mL were collected from the gradients and analyzed by SDS−PAGE (GRP94 samples) or by the absorbance at 280 nm (protein standards).

Determination of Molecular Weight and Quaternary Structure. Based on the experimentally determined parameters for the *s* value and R_s, the native molecular weight (*M*) of proteins was calculated using the following equation (Siegel & Monty, 1966):

$$M\ (\mathrm{Da}) = N(6\pi\eta R_s)s/(1 - \upsilon_2\rho) = 4054s(R_s)$$

where N = Avogadro's number, η is the viscosity of the solvent (0.01 g/cm^3 for water at 20 °C), and $\upsilon_2\rho$ (0.73 cm^3/g) is the partial specific volume. The frictional ratio, f/f_{min}, was calculated from the relationship $f/f_{min} = s_{max}/s$. The s_{max}

for a protein of a given molecular weight was calculated using the equation:

$$s_{max} = M(1 - \upsilon_2\rho)/N(6\pi\eta R_{min}) = (3.75 \times 10^{-16})M^{2/3}$$

Proteolytic Digestion of GRP94. Purified GRP94 (3.5 μg) was digested with a final concentration of 0%, 0.25%, 1.0%, or 5% (w/w) elastase for 30 min at 30 °C in 25 μL of buffer A. Triplicate samples were run on 12.5% SDS−PAGE gels. One set was stained with Coomassie Blue to visualize the digestion products, and the others were transferred to nitrocellulose for immunoblotting. Immunoblotting was performed as described (Wearsch & Nicchitta, 1996) using polyclonal anti-GRP94 antibodies directed against either the N-terminus (Cala & Jones, 1994) or the C-terminus (DU-32). For structural analyses of the N-terminal digestion product, 12 μg of GRP94 was digested with 7.5% elastase (w/w) for 30 min at 30 °C in 75 μL of buffer A. Following the incubation, PMSF (phenylmethanesulfonyl fluoride) was added to a final concentration of 5 mM. The resulting 84 kDa digestion product was analyzed by gel filtration and velocity sedimentation as described above.

Construct Preparation. A plasmid containing the canine GRP94 cDNA cloned into the *Eco*RI restriction site of pBS-SK$^+$ was a generous gift of Dr. Steve Cala (Wayne State University, Detroit, MI). For in vitro expression, GRP94 inserts were placed into pTBU, an expression vector created by replacing the *Hin*dIII−*Eco*RI polylinker region of pGEM-3Z (Promega, Madison, WI) with the *Hin*dIII−*Eco*RI fragment of the polylinker region of pSPUTK (Stratagene, La Jolla, CA).

For in vitro expression studies, the full length coding region of GRP94 (amino acid residues −21 to 783) was cloned into pTBU as two fragments generated by PCR. Canine GRP94 cDNA was used as a template for all PCR reactions. In the first reaction, the 5′ sense primer (5′ GAT CCC ATG GGA AAA GCC CTG TGG GTG CTG 3′) and the 3′ antisense primer (5′ AAT TGT TGT TCC CCG 3′) were used to prepare a PCR product corresponding to the 5′ 750 bp of the GRP94 coding region, but with a novel *Nco*I site at the start codon. In doing so, the arginine residue at amino acid position 2 was replaced with glycine-lysine. This PCR product was digested with *Nco*I/*Nsi*I to generate a fragment corresponding to nucleotides 1−187 of the coding region. In the second PCR reaction, the same 5′ sense primer and the 3′ antisense primer (5′ GGC GAA TTC CCT CTC CAC ACA GG 3′) were used to generate a product corresponding to the entire coding region (1−2415), with a novel *Eco*RI site introduced 18 bp after the termination codon. Digestion of the PCR product with *Nsi*I and *Eco*RI generated a fragment corresponding to the remaining sequence of the GRP94 coding region. The *Nco*I−*Nsi*I and *Nsi*I−*Eco*RI PCR products were ligated with *Nco*I/*Eco*RI-digested pTBU vector to yield the full length clone.

GRP94-ΔC, a construct encoding amino acids 1−600, was made to remove the region encoding the N-terminal signal sequence and the C-terminal 183 amino acid residues. A PCR reaction was performed in which a new start ATG and *Nco*I site were introduced in frame with the first codon of the mature GRP94 sequence using the 5′ sense primer (5′ CGT GCC ATG GAC GAT GAA GTC GAT G 3′) and the 3′ antisense primer (5′ AAT TGT TGT TCC CCG 3′). This PCR product was digested with *Nco*I/*Nsi*I to generate a 5′ fragment of GRP94 lacking the signal sequence (nucleotides 67−187 of the coding region). In a second PCR reaction, the same 5′ sense primer and the 3′ antisense primer (5′ CGT GTC GAC AGT TGA GCA GAG GCT C 3′) were used to generate a product corresponding to the coding region encompassed by nucleotides 67−1960. This PCR reaction also introduced a *Sal*I site at position 1960 of the product, yielding a substitution of the tryptophan codon with that of cysteine. Digestion of this PCR product with *Nsi*I and *Sal*I generated a fragment corresponding to the remaining 3′ sequence of GRP94, but lacking the region coding for the C-terminal 183 amino acids. The *Nco*I−*Nsi*I and *Nsi*I−*Sal*I PCR products were ligated into *Nco*I/*Sal*I digested pTBU.

GRP94-Cexp encodes the C-terminal 200 amino acids of GRP94 (584−783) and was prepared as follows. A PCR reaction using the 5′ sense primer (5′ GAG TCC ATG GAG AGT CGT GAA GCG 3′) and the 3′ antisense primer (5′ GGC GAA TTC CCT CTC CAC ACA GG 3′) was performed, yielding a product in which the sequence encoding a lysine at amino acid 584 was changed to a methionine via incorporation of an *Nco*I site. The PCR product was digested with *Nco*I/*Eco*RI and cloned into *Nco*I/*Eco*RI digested pTBU.

The construct MBP-94C is a fusion of the C-terminal 108 amino acids (676−783) of GRP94 at the C-terminus of MBP (maltose binding protein) and was prepared by PCR using the 5′ sense primer (5′ GCG GAT CCA TGC TGC GAC GAG T 3′) and the 3′ antisense primer (5′ CGC TGC AGC CCT CTC CAC ACA GG 3′). In this construct, a *Bam*HI and a *Pst*I site are present at the 5′ and 3′ ends of the clone, respectively. The *Bam*HI/*Pst*I digested PCR fragment was cloned into the polylinker region of the pMAL-c2 vector (New England Biolabs, Beverly, MA) in frame with the MBP sequence and transformed into BL21 competent cells.

To further map the region of the C-terminus that contained the assembly domain, the constuct MBP 676−719 was made to express the GRP94 C-terminal hydrophobic domain as a fusion with MBP. PCR using the 5′ sense primer (5′ GCG GAT CCA TGC TGC GAC GAG T 3′) and the 3′ antisense primer (5′ GCC TGC AGT TAT TCT ATT CGA TCT CC 3′) generated a fragment encoding amino acids 676−719 with a novel *Bam*HI site at the 5′ end as well as a stop codon and novel *Pst*I site at the 3′ end. *Bam*HI−*Pst*I digested PCR product was ligated into *Bam*HI−*Pst*I digested pMAL-c2 vector. MBP 713−783 is an MBP fusion encoding the C-terminal sequence subsequent to the hydrophobic domain. PCR with the 5′ sense primer (5′ GCG AAT TCG CAT ATG GAG ATC GA 3′) and the 3′ antisense primer (5′ CGC TGC AGC CCT CTC CAC ACA GG 3′) yielded a product that was digested with *Eco*RI and *Pst*I and cloned into the appropriate sites in the pMAL-c2 vector.

In Vitro Transcription and Translation. The plasmids containing the full length GRP94 cDNA and GRP94-Cexp inserts in pTBU were digested with *Eco*RI. Transcription reactions were performed with 10 μg of linearized DNA, in a buffer consisting of 40 mM Tris-HCl, pH 8.0, 8 mM $Mg(OAc)_2$, 25 mM NaCl, 2 mM spermidine, 10 mM DTT, 2.5 mM ATP, CTP, GTP, and UTP, 5 U/mL yeast inorganic phosphatase, and 1 U/μL T7 RNA polymerase for 3 h at 37 °C. Translation reactions, in a final volume of 20 μL, contained 0.5−1.0 μg of the appropriate mRNA, 20 units of RNasin, 8 μL of nuclease-treated reticulocyte lysate, and 25 μCi of ^{35}S Pro-Mix (methionine plus cysteine) in a buffer

adjusted to a final concentration of 1 mM DTT, 100 mM KCl, and 1 mM $MgCl_2$. Translation reactions were performed at 30 °C for 1 h. Where indicated, canine pancreatic microsomes (1 equiv) were included in the translation and, following the incubation, were recovered by centrifugation of the translation reaction over a sucrose cushion (0.5 M sucrose, 25 mM K-Hepes, pH 7.2, 1 mM DTT) at a ratio of 3:1 (supernatant:cushion) for 10 min at 60 000 rpm, 4 °C, using the Beckman TLA100 rotor. Microsomes were detergent permeabilized with 0.25% Nikkol for 20 min on ice. GRP94 translation products were recovered in the supernatant after a second centrifugation step.

Recombinant Expression and Purification of MBP Fusion Proteins. BL21 transformants carrying the pMAL-c2 plasmid with the indicated GRP94 inserts were grown at 37 °C to a density of $A_{600} = 0.5$, in a culture volume of 0.5 L. Expression (1.5 h at 30 °C) was induced by the addition of IPTG to a final concentration of 0.1 mM. The cells were collected by centrifugation at 4000*g* for 20 min at 4 °C, and the cell pellet was resuspended in 50 mL of 10 mM sodium phosphate, pH 7.2, 50 mM NaCl, and 1 mM DTT. Lysozyme was added to a final concentration of 0.2 mg/mL, and following a 20 min incubation on ice, deoxycholate was added to a final concentration of 0.4 mg/ml. After a brief sonication, the cell lysate was recovered following centrifugation at 8000*g* for 10 min. The cell lysate was diluted 1:3 in buffer to yield a final concentration of 10 mM sodium phosphate, pH 7.5, 500 mM NaCl, 0.25% Tween-20, and 1 mM DTT, and incubated with 2.5 mL of a 50% slurry of amylose resin for 16 h at 4 °C. The resin was washed twice with 5 mL of 10 mM sodium phosphate, pH 7.2, 500 mM NaCl, and 1 mM DTT, and the fusion protein was eluted with 0.5 mL of buffer B (10 mM maltose, 10 mM sodium phosphate, pH 7.2, 500 mM NaCl, 1 mM DTT). Factor Xa cleavage of the fusion protein was performed using 2% (w/w) protease in buffer B at 4 °C for 24 h.

Electron Microscopy. Purified GRP94 (150 μg) was incubated in the presence or absence of 1% elastase (w/w) for 15 min at 30 °C. Full length GRP94 and the 84 kDa digestion product were subsequently purified by centrifugation on 15−40% glycerol gradients supplemented with 0.1 M ammonium bicarbonate in the Beckman SW50 rotor at 45 000 rpm for 15 h at RT. Fractions were collected from the gradients and analyzed by SDS−PAGE to confirm the purity of the sample. The protein containing fractions (10 μL) were prepared for rotary shadowing electron microscopy as described in Fowler and Erickson (1979).

RESULTS

Hydrodynamic Properties of Native GRP94. Previously we reported that, by native gel electrophoresis, GRP94 behaves as a dimer of noncovalently associated subunits (Wearsch and Nicchitta, 1996). On preparative gel filtration, however, GRP94 eluted with an apparent molecular weight of 600 kDa (Wearsch & Nicchitta, unpublished observations). These two observations can be reconciled should the protein be distinctly nonglobular in shape. To gain insight into the relative shape and hydrodynamic properties of GRP94, the Stokes radius (R_s) and sedimentation coefficient (*s*) were determined for the native protein (Figure 1). The elution volume of GRP94 by analytical gel filtration corresponded to an R_s of 7.4 nm (Figure 1A), and velocity sedimentation

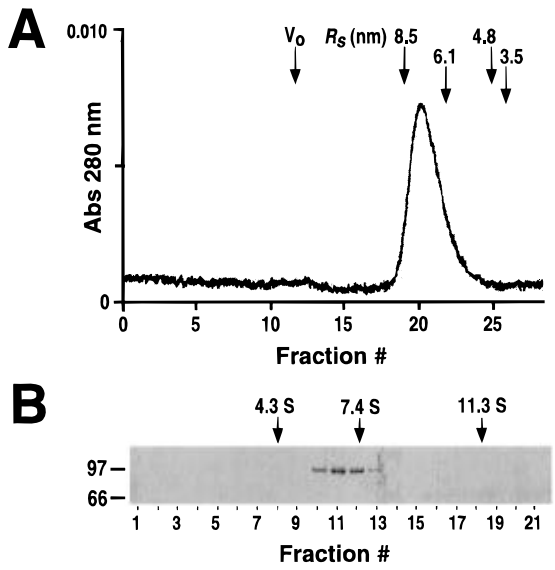

Rs (nm)	Sed. Coeff.	Oligomer. State	Native MW (kDa)	*f/fmin*
7.4	6.7 S	dimer	200	1.9

FIGURE 1: Structural analysis of native GRP94. The hydrodynamic properties of native GRP94 were characterized by gel filtration chromatography and velocity sedimentation. (A) Analytical gel filtration chromatography. The elution profile of native GRP94 was monitored by the absorbance at 280 nm. Arrows indicate the elution position and Stokes radius (R_s) of the protein standards (thyroglobulin, 8.5 nm, 660 kDa; apoferritin, 6.1 nm, 440 kDa; aldolase, 4.8 nm, 160 kDa; BSA, 3.5 nm, 66 kDa). (B) Velocity sedimentation. Native GRP94 was analyzed by centrifugation on 15−30% sucrose gradients. Fractions of 0.5 mL were collected and analyzed by SDS−PAGE. Fraction #1 represents the top of the gradient and fraction #21 represents the bottom. Arrows indicate the position and *s* values of the protein standards (BSA, 4.3 S; yeast alcohol dehydrogenase, 7.4 S; catalase, 11.3 S). The predicted molecular weight and frictional ratio (f/f_{min}) were calculated as described in the Experimental Procedures.

yielded an *s* value of 6.7 S (Figure 1B). The native molecular weight of GRP94 was calculated according to Siegel and Monty (1966) (see Experimental Procedures) and was determined to be 200 kDa. This indicated that GRP94 exists as a dimer of 100 kDa subunits, in agreement with previous reports (Koyasu et al., 1986; Wearsch & Nicchitta, 1996). The frictional ratio (f/f_{min}), calculated from the relationship $s_{max}/s = f/f_{min}$, was used to make predictions on the shape of the molecule. GRP94 was found to have a frictional ratio of 1.9, indicating that the protein has a distinctly nonglobular shape. This finding readily explains the unexpectedly large apparent molecular weight determined by gel filtration and suggests that the protein has an elongated structure.

Detergent-Induced Monomerization of GRP94. Hydrophobic interactions commonly provide the primary energetic contribution to subunit assembly in oligomeric proteins, and thus, for many oligomeric proteins, subunit dissociation can be induced upon addition of detergent (Janin & Chothia, 1990; Mignery et al., 1990; Shen et al., 1993). To examine the role of hydrophobic interactions in the oligomeric assembly of GRP94, the native protein was incubated in the presence of Zwittergent 3-12 for 45 min at RT and then analyzed by gel filtration chromatography (Table 1). This treatment resulted in a shift of the dimeric species to a fraction eluting with an R_s of 5.8 nm. Velocity sedimentation

Table 1: Hydrodynamic Properties of Zwittergent 3-12-Treated GRP94 Constructs

	GRP94	GRP94-Cexp	MBP-94C
R_s (nm)	5.8	3.4	4.9
sedimentation coeff (S)	4.2	ND[a]	ND[a]
mol wt (kDa)	100	23	52
oligomerization state	monomer	monomer	monomer

[a] ND = not determined.

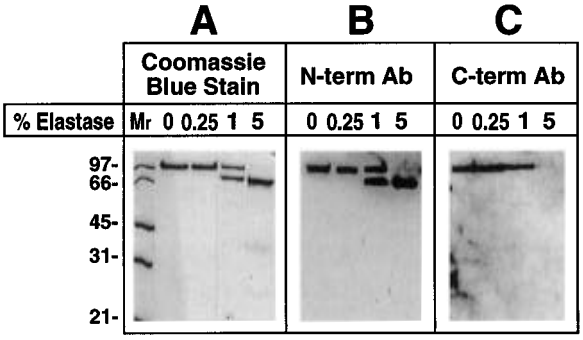

FIGURE 2: Protease mapping of GRP94. Purified GRP94 (3.5 μg) was digested with the indicated concentrations of elastase for 30 min at 30 °C and analyzed by SDS−PAGE. (A) Coomassie Blue stain of the GRP94 digestion products. (B) Immunoblot of the digestion products using an anti-peptide antibody generated against the N-terminal 14 amino acids of GRP94. (C) Immunoblot of the digestion products using an anti-peptide antibody generated against the C-terminal 44 amino acids of GRP94.

analysis of the Zwittergent 3-12 shifted fraction yielded an *s* value of 4.2 S (Table 1). These values are in agreement with the Zwittergent 3-12 dependent generation of 100 kDa monomers. Removal of the detergent, by addition of the detergent binding resin Calbiosorb, resulted in reassembly of the monomers into dimers, as assayed by gel filtration (data not shown). These results suggest that hydrophobic interactions likely contribute to GRP94−GRP94 subunit interactions.

Identification of Subunit Assembly Domain. Members of the hsp90 family of molecular chaperones, including GRP94, exhibit a high degree of sequence conservation (Gupta, 1995) and have been found to exist predominantly as dimers (Koyasu et al., 1986; Spence & Georgopoulos, 1989; Minami et al., 1991). In view of the well conserved aspects of both amino acid sequence and quaternary structure, it would be expected that the dimeric state is intimately related to cellular function. To identify potential oligomerization domains, we employed a protease mapping approach. GRP94 was incubated with increasing amounts of elastase for 30 min at 30 °C, and the digestion pattern was analyzed by SDS−PAGE (Figure 2). Coomassie Blue staining of the digestion products revealed a single predominant limit digestion product with a relative mobility of 84 kDa on SDS−PAGE (Figure 2A). To map the proteolysis site(s), the digestion products were transferred to nitrocellulose and probed with antibodies directed against either the N-terminal 14 amino acids or the C-terminal 44 amino acids of GRP94. Immunoreactivity of the 84 kDa digestion product with the N-terminal (Figure 2B) but not the C-terminal antibody (Figure 2C) indicated that approximately 16 kDa was removed from the C-terminus. No limit digestion products corresponding to the proteolyzed C-terminal domain were identified. Similar digestion patterns of GRP94 were observed using trypsin, chymotrypsin, and thermolysin, suggesting that this region

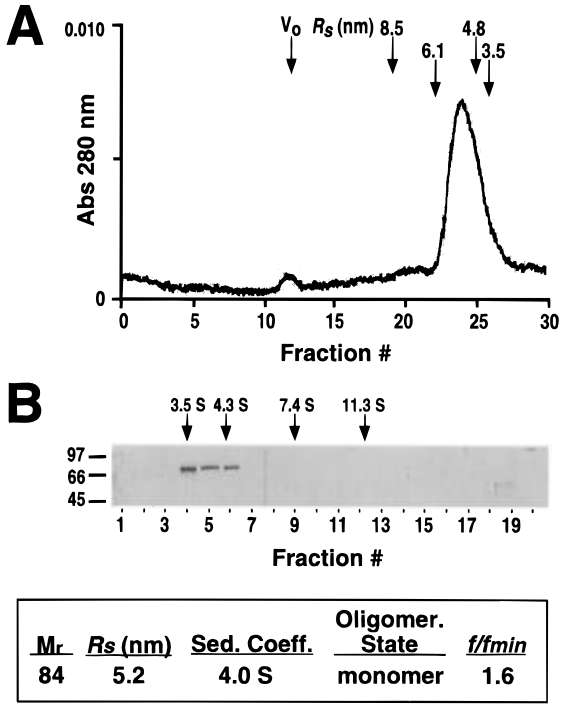

FIGURE 3: Structural analysis of the GRP94 84 kDa digestion product. GRP94 (12 μg) was digested with 7.5% elastase (w/w) for 30 min at 30 °C and analyzed for its oligomerization state. (A) Analytical gel filtration chromatography. The elution profile of the 84 kDa digestion product was monitored by the A_{280} and analyzed as described in the legend to Figure 1. (B) Velocity sedimentation. The 84 kDa digestion product was analyzed by centrifugation on 15−30% sucrose gradients. Fractions of 0.5 mL were collected and analyzed by 12.5% SDS−PAGE. Arrows above indicate the peaks and *s* values of the protein standards (ovalbumin, 3.5 S; BSA, 4.3 S; yeast alcohol dehydrogenase, 7.4 S; catalase, 11.3 S).

is hypersensitive to proteolysis and thus may represent a structural domain junction (data not shown).

To determine whether proteolytic removal of the C-terminal 16 kDa of GRP94 affected the oligomerization state, the N-terminal digestion product was analyzed by gel filtration chromatography and velocity sedimentation. The N-terminal digestion product was identified as a single species possessing an R_s of 5.2 nm (Figure 3A) and an *s* value of 4.0 S (Figure 3B). This dramatic change in the hydrodynamic behavior relative to native GRP94 is consistent with the disassembly of the protein into monomers of 84 kDa. However, from these data it is not certain whether the protease-induced monomerization reflected the loss of an assembly domain, or alternatively, whether it is an epiphenomenon reflecting denaturation or structural disruption of an assembly domain from a distant site.

In Vitro Assembly of GRP94. To study the role of the C-terminal domain of GRP94 in oligomeric assembly, an experimental system was developed to analyze assembly in vitro. Full length GRP94 mRNA was translated in rabbit reticulocyte lysate supplemented with [^{35}S]methionine and pancreatic rough microsomes for 1 h at 30 °C. Translation reactions were supplemented with rough microsomes to allow assembly of GRP94 in its native environment. Microsomes were recovered from the translation mixture by centrifugation through a sucrose cushion and permeabilized with detergent to release the lumenal protein fraction. A doublet of GRP94 translation products was observed by SDS−PAGE (Figure 4). Treatment of the translation products with endoglycosi-

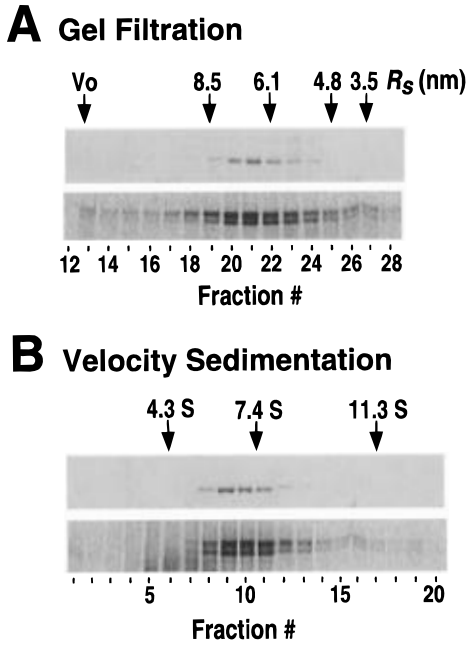

FIGURE 4: In vitro assembly of full length GRP94. mRNA encoding the full length GRP94 sequence (amino acids −21 to 783) was translated in reticulocyte lysate in the presence of [^{35}S]methionine and canine pancreatic microsomes for 1 h at 30 °C. Microsomes were recovered by centrifugation of the translation reaction over a 0.5 M sucrose cushion and then detergent permeabilized with 0.25% Nikkol. The released lumenal protein pool was analyzed by gel filtration chromatography (A) and velocity sedimentation (B), in parallel with native GRP94. Fractions of 0.5 mL were collected and analyzed by SDS−PAGE. The upper gels in each panel show the Coomassie stain for the native GRP94 fractions, and the lower gels show the phosphorimage of the in vitro synthesized GRP94 fractions. Arrows indicate the R_s and s values of the gel filtration and sucrose gradient standards, respectively.

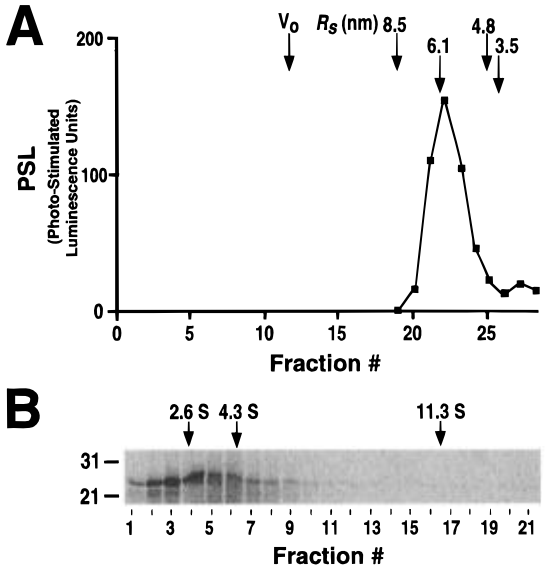

R_S (nm)	Sed. Coeff.	Oligomer. State	Native MW (kDa)	f/f_{min}
6.0	1.9 S	dimer	46	2.5

FIGURE 5: Analysis of the assembly activity of the C-terminal 200 amino acids in vitro. GRP94-Cexp (corresponding to amino acids 584−783) was expressed in reticulocyte lysate with [^{35}S]methionine for 1 h at 30 °C and analyzed for its oligomerization state. (A) Analytical gel filtration chromatography. Fractions of 0.5 mL were collected, and the elution profile GRP94-Cexp translation products were determined by SDS−PAGE. The graph represents the phosphorimager-based quantitation of the bands in each fraction. (B) Velocity sedimentation. GRP94-Cexp translation products were analyzed by centrifugation on 10−25% sucrose gradients. Fractions of 0.5 mL were collected from the gradient, analyzed by SDS−PAGE, and detected using the phosphorimager. Arrows indicate the peaks for the protein standards with their s values (chymotrypsinogen A, 2.6 S; BSA, 4.3 S; catalase, 11.3 S). The oligomerization state was determined based on a molecular weight of 23 kDa per subunit.

dase H yielded a single band, indicating that in vitro synthesized GRP94 was comprised of differentially glycosylated species (data not shown). To analyze the assembly state of the translation products, the lumenal protein fraction was subsequently analyzed by gel filtration chromatography and velocity sedimentation in parallel with native GRP94 (Figure 4). The GRP94 translation products exhibited an identical profile with that of native GRP94 by gel filtration (R_s = 7.4 nm, Figure 4A) as well as velocity sedimentation (s = 6.7 S, Figure 4B). Within the experimental limits of these analyses, we conclude that in vitro synthesized GRP94 assembles into a state that is structurally identical to the native dimer.

To determine if oligomeric assembly of GRP94 required the physical/chemical environment of the ER lumen, the assembly of a GRP94 construct lacking the N-terminal ER signal sequence was analyzed. In the absence of translocation, approximately 65% of the GRP94 translation products were able to assemble into dimers, suggesting that modifications characteristic of the ER lumen, such as N-linked glycosylation, are not essential for assembly (data not shown). Thus, an in vitro translation system lacking ER membranes can be used to further analyze the assembly reaction.

Requirement of the C-Terminal Domain for Assembly in Vitro. Having established an in vitro system that supports translation and oligomerization of GRP94, the role of the C-terminal domain in cotranslational subunit assembly was analyzed. To determine if this domain was necessary for dimerization, a construct (GRP94-ΔC) was made lacking both the N-terminal signal sequence and the C-terminal 20 kDa, approximately the region removed by proteolysis of the native protein. GRP94-ΔC mRNA was expressed in reticulocyte lysate, and the translation products were determined to be monomeric, with an R_s of 5.2 nm and s value of 3.7 S (data not shown). The hydrodynamic properties for the GRP94-ΔC translation products were nearly identical to those of 84 kDa digestion product (Figure 3). These results demonstrate that the C-terminal domain is essential for dimerization of de novo synthesized GRP94 and are consistent with the localization of the assembly domain to this region of the protein.

GRP94-Cexp, a construct encoding the C-terminal 200 amino acids of GRP94, was used to determine if the C-terminal domain alone was sufficient for oligomerization. Following translation in reticulocyte lysate, GRP94-Cexp translation products were analyzed by gel filtration chromatography and velocity sedimentation (Figure 5). Although the predicted molecular weight based on the amino acid sequence of GRP94-Cexp is 23 kDa, the gel filtration profile indicated a peak for the translation products at a particularly large R_s of 6.0 nm (Figure 5A) and eluting near apoferritin (R_s = 6.0 nm, MW = 440 kDa). This observation initially suggested that GRP94-Cexp may exist as large oligomers. However, based on the s value of 1.9 S (Figure 5B), the

native molecular weight of GRP94-Cexp was calculated to be approximately 46 kDa, indicating that the translation products were, in fact, assembled into dimers. The large frictional ratio of 2.5 reflects the highly elongated shape of the GRP94-Cexp dimers. Similar to native GRP94, treatment of GRP94-Cexp dimers with 4 mM Zwittergent 3-12 resulted in dissociation into monomers, with an R_s of 3.4 nm (Table 1). These findings further map the assembly domain within the C-terminal 200 amino acids of GRP94 and demonstrate that this region is both necessary and sufficient for assembly in vitro.

Demonstration of Autonomous Assembly Activity in Vivo. Having determined that the C-terminal 200 amino acids of GRP94 were capable of autonomous assembly in vitro, it was of interest to analyze assembly in vivo and map to a higher resolution the C-terminal region possessing dimerization activity. As noted previously, dissociation of both native and GRP94-Cexp dimers by Zwittergent 3-12 suggests that hydrophobic interactions contribute to the assembly process. Within the C-terminal 200 amino acid domain, the only substantially hydrophobic region is located at amino acids 692−709. Using recombinant expression in *E. coli*, amino acids 676−783 of GRP94 were thus tested for the ability to direct the dimerization of maltose binding protein (MBP), a 42 kDa monomer.

MBP-94C was created by placing the sequence encoding the C-terminal 108 amino acids of GRP94 in frame and at the C-terminus of MBP. The fusion protein was expressed in *E. coli* host strain BL21 and purified using amylose affinity chromatography. Gel filtration was used to compare the oligomerization states of MBP and MBP-94C. MBP is a globular monomer with a R_s of approximately 3.0 nm (Figure 6A). The elution profile of MBP-94C (54 kDa) showed a dramatic shift in the R_s to 8.3 nm, an elution position approximating that of thyroglobulin (8.5 nm, 660 kDa; Figure 6B). Velocity sedimentation experiments yielded an *s* value of 3.3 S (data not shown), indicating that MBP-94C exists as a dimer with a native molecular weight of 108 kDa. The unusually large R_s for a protein of this size is reflected in the f/f_{min} of 2.5, indicating that the GRP94 C-terminal domain conferred an elongated shape to the fusion protein. To determine whether the apparent dimerization activity was strictly limited to the GRP94-derived C-terminal domain, the fusion protein was digested with factor Xa protease to cleave the linker domain, and the hydrodynamic properties were re-evaluated. Gel filtration analysis of the factor Xa released MBP yielded an elution profile identical to that of MBP (Figure 6A,C), confirming that dimerization is taking place through the GRP94 domain. In addition, treatment with Zwittergent 3-12 completely dissociated MBP-94C dimers into monomers, consistent with previous observations (Table 1).

To further map the assembly domain within the C-terminal 108 amino acids, the role of the hydrophobic sequence, located at amino acids 692−709, in the regulation of assembly was determined. Two additional GRP94−MBP fusions were made: MBP 676−719 (47 kDa), which includes the hydrophobic domain and the immediate flanking regions, and MBP 713−783 (50 kDa), which corresponds to the domain extending from hydrophobic region to the C-terminus. MBP 713−783, eluting near MBP by gel filtration, behaved as a monomer with an R_s of 3.4 nm (Figure 6D), indicating that the domain C-terminal to the hydrophobic

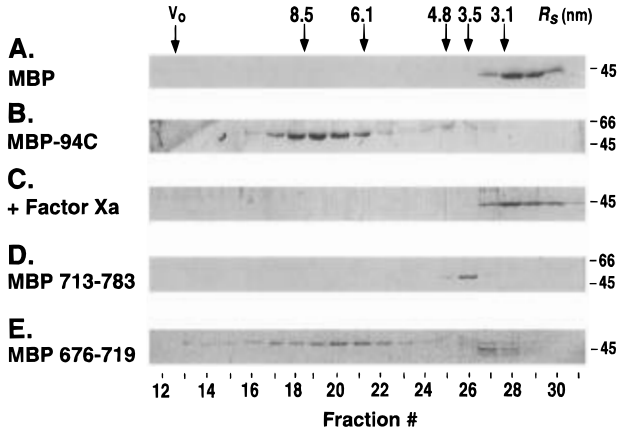

	Rs (nm)	Sed. Coeff.	Oligomer. State	Native MW (kDa)	*f/fmin*
MBP	3.0	ND	monomer	42	ND
MBP-94C	8.3	3.3 S	dimer	108	2.5
MBP 676-719	7.1	3.4 S	dimer	94	2.3
MBP 713-783	3.4	ND	monomer	50	ND

FIGURE 6: Fusion of GRP94 to MBP and assembly in vivo. GRP94 C-terminal sequences were expressed as fusions with MBP, purified by amylose affinity chromatography, and analyzed by gel filtration chromatography. Fractions of 0.5 mL were collected and analyzed by SDS−PAGE and Coomassie Blue staining. (A) MBP standard. (B) MBP-94C (amino acids 676−783 of GRP94). (C) MBP-94C treated with 2% factor Xa protease (w/w) for 24 h at 4 °C. (D) MBP 713−783. (E) MBP 676−719. The native molecular weight for MBP fusions was calculated from the R_s determined from the elution volume (above) and the *s* value obtained from velocity sedimentation (data not shown). Oligomerization states were determined based on the molecular weight predicted by the amino acid sequence: MBP-94C, 54 kDa; MBP 676−719, 47 kDa; MBP 713−783, 50 kDa.

sequence is incapable of autonomous oligomerization. In contrast, the profile of MBP 676−719, which includes the hydrophobic domain, eluted similarly to MBP-94C in a somewhat broad peak centered at an R_s of 7.1 nm (Figure 6E). In combination with the *s* value of 3.4 S obtained from velocity sedimentation studies (data not shown), it was determined that MBP 676−719 was predominantly assembled into dimers. The second peak for MBP 676−719, eluting near MBP, represents proteolyzed and unassembled monomers. Similar to native GRP94 and MBP-94C, MBP 676−719 dimers possess a large f/f_{min} of 2.3, indicating that the dimerization event, although in the context of a fusion protein, produces a highly extended structure. These results identify a functional, autonomous assembly domain located within the C-terminal amino acids 676−719 of GRP94 which is necessary and sufficient for dimerization in vivo.

Electron Microscopy of Native and Protease-Digested GRP94. To further develop a structural model, rotary shadowing electron microscopy was used to visualize the shape and determine the molecular dimensions of GRP94. As shown in Figure 7A, native GRP94 is composed of three distinct, nodular domains and is found in both rod-like and "wing" conformations. The rod-like structures were determined to have molecular dimensions of an average length of 27.8 nm and width of 6.8 nm, dimensions consistent with the hydrodynamic data and the calculated f/f_{min}. Having identified the GRP94 assembly domain near the C-terminus, the shape and dimensions of the monomeric N-terminal protease digestion product were also determined (Figure 7B).

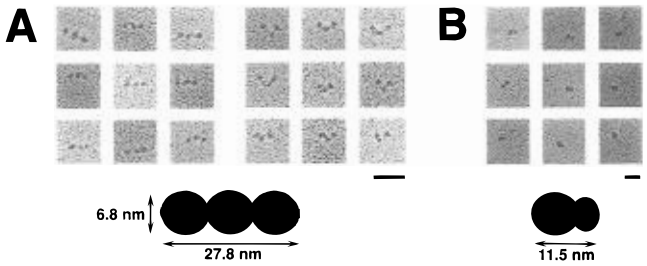

FIGURE 7: Electron microscopy of GRP94. Samples were purified on 10−40% glycerol gradients supplemented with 0.1 M ammonium bicarbonate and prepared for electron microscopy by rotary shadowing. (A) Native full length GRP94. Bar = 50 nm. Molecules were identified as rods (left panel) and wings (right panel). (B) N-Terminal 84 kDa digestion product generated by treatment of 150 μg of GRP94 with 1% elastase for 15 min at 30 °C. Bar = 25 nm. The diagrams below illustrate the structures observed by electron microscopy and their average molecular dimensions.

These molecules, lacking the C-terminal 16 kDa, had a slightly irregular shape and were composed of one complete nodular domain with a small, tail-like structure. The average length of the monomeric molecules was 11.5 nm, slightly less than half of the length of native GRP94. These data support a tail-to-tail orientation of the subunits, placing the C-terminal assembly domains interacting within the central domain of a trinodular dimer.

DISCUSSION

Hydrodynamic studies of recombinant fusion protein fragments of GRP94 have allowed the identification of a discrete domain, defined by residues 676−719, which mediates the obligatory dimeric assembly of GRP94 in vivo and in vitro. This domain displays autonomous assembly activity and confers the characteristic extended, rod-like conformation of the native protein to fusion protein constructs. On the basis of these findings, and the observation that native GRP94 and GRP94 C-terminal domain constructs can be dissociated into monomers upon treatment with the detergent Zwittergent 3-12, we propose that the hydrophobic region corresponding to amino acids 692−709 is the primary subunit−subunit interface. This assignment is consistent with the observation that subunit interfaces in oligomeric proteins tend to be of relatively high hydrophobicity (Janin & Chothia, 1990). It should be noted that the elution profile of MBP 616−719 on gel filtration is somewhat broader than that observed for MBP-94C, suggesting that although the hydrophobic domain is necessary and sufficient for dimerization, the efficiency of assembly may be influenced by flanking regions.

A structural model was compiled from the results of this study and is depicted in Figure 8. GRP94 is illustrated as a trinodular rod composed of three domains. The interaction of the subunits at their respective C-termini yields the central domain and provides for an opposed orientation of the two subunits. This tail-to-tail orientation is consistent with the localization of the assembly domain to the C-terminus by protease mapping and the dramatic alterations in the hydrodynamic behavior of MBP which accompany its expression as a GRP94 assembly domain fusion. Direct evidence for a tail-to-tail orientation is provided by the rotary shadowing electron micrographs (Figure 7). By rotary shadowing EM, the native GRP94 dimer was identified as a trinodular molecule of approximately 28 nm in length (Figure 7A) and

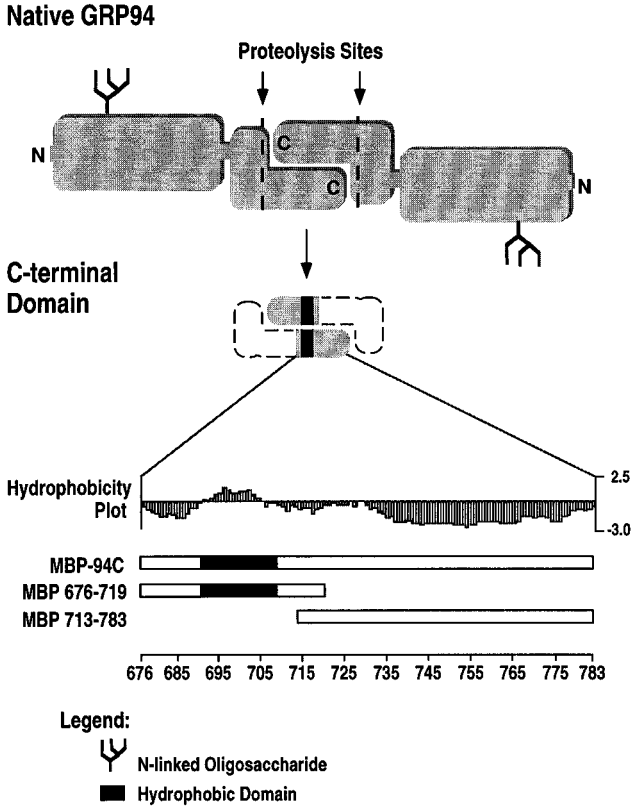

FIGURE 8: Structural model of GRP94. In its native state, GRP94 is an elongated, opposed dimer consisting of three structural domains. Subunit interaction occurs in the central of the three domains. GRP94 is hypersensitive to proteolysis in the central domain, which removes the assembly domain from the remaining N-terminal digestion product. A hydrophobicity plot of the C-terminal 108 amino acids indicates the presence of a single hydrophobic domain (represented by the black box) between amino acids 692−709 of GRP94 followed by a highly charged acidic domain. The hydrophobic region was required and sufficient for dimerization of MBP−GRP94 fusions, indicated below. Hydrophobicity was calculated using the method of Kyte and Doolittle.

the monomeric, protease-derived 84 kDa fragment as a molecule of 11−12 nm, roughly one-half the length of the intact dimer (Figure 7B). These data provide a compelling structural argument for an opposed orientation of the two subunits.

The data reported herein indicate that GRP94 is similar to its cytosolic homolog hsp90 in both oligomerization state (dimer) and site of assembly (C-terminus) (Koyasu et al., 1986; Ianotti et al., 1988; Minami et al., 1991; Nemoto et al., 1995). Given the relatively high degree of sequence conservation between members of this family, it is not unexpected that the oligomerization domain may be conserved between hsp90 family members. There are, however, fundamental differences in the regulation of assembly between the cytosolic and ER hsp90's that belie the high degree of sequence conservation. Perhaps most significantly, although the C-terminal 15 kDa regions of the α and β forms of hsp90 are highly homologous (>85% identity), the β isoform has been shown to exist in both monomer and dimer forms (Minami et al., 1991). The C-terminal 12 kDa region of GRP94 diverges substantially from hsp90α/β, (<40% identity) yet, like hsp90α, is an obligatory dimer. Furthermore, although a hydrophobic domain similar to that observed for GRP94 is also present in hsp90α and β, the minimal assembly domain described in this study does not

coincide with the assembly domain reported for hsp90α (Nemoto et al., 1995). Further mapping of the dimerization domain of hsp90α/β should provide insight into the molecular regulation of assembly of the two proteins.

No function has yet been ascribed to the N-terminal region, which contains the areas of highest sequence homology between the hsp90 family members (Gupta, 1995). It is of interest to note that the putative ATP binding domains of GRP94 have been identified within these regions (Figure 8). Similar to hsp90, ATP binding activity, as well as very low basal ATPase activity, has been reported for GRP94 (Csermely & Kahn, 1991; Nadeau et al., 1993; Clairmont et al., 1992; Li & Srivastava, 1993). However, recent evidence indicates that the ribonucleotide binding and hydrolysis activity reported for hsp90 is a consequence of contamination, and not reflective of an inherent property of the protein (Ianotti et al., 1988; Jakob et al., 1996). By inference, the chaperone function of GRP94 is also likely to be ATP independent, and thus the hsp90 chaperones may function in a manner similar to nucleotide-independent chaperones, such as PapD (Kuehn et al., 1993).

The identification of a defined domain which mediates the obligatory assembly of GRP94 establishes an experimental system for future studies on the structural basis of GRP94 function. In this regard, it should be again noted that the assembly domain defined by residues 676−719 confers an extended, opposed structural alignment to the two subunits. This is in marked contrast to the other prominent ER chaperone BiP, a member of the hsp70 family of stress proteins. BiP is a globular protein composed of two functional domains, a peptide binding domain with a marked preference for hydrophobic sequences and an ATP binding domain, which mediates ATP binding and hydrolysis. By analogy to its bacterial homolog DnaK, BiP contains a single peptide binding site per molecule and is active as a monomer (Chappel et al., 1987; Zhu et al., 1996; Blond-Elguindi et al., 1993b). GRP94 has been identified as a peptide binding protein in indirect assays measuring the transfer of bound peptides to MHC class I molecules (Arnold et al., 1995; Suto & Srivastava, 1995). At present, little is known concerning the localization or binding specificity of the GRP94 peptide binding site(s). An intriguing possibility, in view of the extended dimeric structure, is that should putative peptide binding sites be located in the N-terminal regions, GRP94 may have the capacity either to bind substrates in a binary manner, or to interact with and "bridge" spatially discrete regions of protein substrate(s). Such binding properties could be particularly valuable for assisting oligomeric assembly reactions. It is therefore noteworthy that, to date, GRP94 has only been found in association with proteins which undergo oligomeric assembly, such as immunoglobulins, MHC class II molecules, collagen, and thyroglobulin (Melnick et al., 1992; Schaiff et al., 1992; Ferreira et al., 1994; Kuznetsov et al., 1994). The ability of full length, dimeric human hsp90α, but not a monomeric C-terminal 49 amino acid truncation, to complement the lethality of *hsp82/hsc82* double mutant strains of *Saccharomyces cerevisiae* further suggests that dimerization is essential for the chaperone activity of hsp90 proteins (Minami et al., 1994). In light of these findings, analysis of assembly-deficient GRP94 may provide intriguing insights into the function of GRP94 in vivo.

ACKNOWLEDGMENT

We thank Edwin C. Murphy III for critical comments on the manuscript and W. Stressman for the isolation of porcine pancreas. We are greatly indebted to Dr. Harold Erickson and Carmen Lucchaveche for their generous assistance with sample preparation and valubale analyses of electron micrographs. We also thank Dr. Steven Cala (Wayne State University, Detroit, MI) for the gift of the GRP94 antibodies and cDNA clone.

REFERENCES

Arnold, D., Faath, S., Rammensee, H.-G., & Schild, H. (1995) *J. Exp. Med. 182*, 885−889.

Blond-Elguindi, S., Cwirla, S. E., Dower, W. J., Lipshutz, R. J., Sprang, S. R., Sambrook, J. F., & Gething, M.-J. (1993a) *Cell 75*, 717−728.

Blond-Elguindi, S., Fourie, A. M., Sambrook, J. F., & Gething, M.-J. (1993b) *J. Biol. Chem. 268*, 12730−12735.

Brodsky, J. L., Goeckler, J., & Schekman, R. (1995) *Proc. Natl. Acad. Sci. U.S.A. 92*, 9643−9646.

Cala, S. E., & Jones, L. R. (1994) *J. Biol. Chem. 269*, 5926−5931.

Chappell, T. G., Konforti, B. B., Schmid, S. L., & Rothman, J. E. (1987) *J. Biol. Chem. 262*, 746−751.

Clairmont, C. A., De Maio, A., & Hirschberg, C. B. (1992) *J. Biol. Chem. 267*, 3983−3990.

Creighton, T. E., Hillson, D. A., & Freedman, R. B. (1980) *J. Mol. Biol. 142*, 43−62.

Csermely, P., & Kahn, C. R. (1991) *J. Biol. Chem. 266*, 4943−4950.

Farquhar, R., Honey, N., Murant, S. J., Bossier, P., Schultz, L., Montgomery, D., Ellis, R. W., Freedman, R. B., & Tuite, M. F. (1991) *Gene 108*, 81−89.

Ferreira, L. R., Norris, K., Smith, T., Heber, C., & Sauk, J. J. (1994) *J. Cell. Biochem. 56*, 518−526.

Flynn, G. C., Chappel, T. G., & Rothman, J. E. (1989) *Science 245*, 385−390.

Flynn, G. C., Pohl, J., Flocco, M. T., & Rothman, J. E. (1991) *Nature (London) 353*, 726−730.

Fourie, A. M., Sambrook, J. F., & Gething, M.-J. (1994) *J. Biol. Chem. 269*, 30470−30478.

Fowler, W. E., & Erickson, H. P. (1979) *J. Mol. Biol. 134*, 241−249.

Fra, A., & Sitia, R. (1993) *Subcell. Biochem. 21*, 143−168.

Freedman, R. B., Hawkins, H. C., Murant, S. J., & Reid, L. (1988) *Biochem. Soc. Trans. 16*, 96−99.

Gething, M.-J., & Sambrook, J. (1992) *Nature (London) 355*, 33−45.

Gragerov, A., & Gottesman, M. E. (1994) *J. Mol. Biol. 241*, 133−135.

Gunther, R., Srinivasan, M., Haugejorden, S., Green, M., Ehbrecht, I. M., & Kuntzel, H. (1993) *J. Biol. Chem. 268*, 7728−7732.

Gupta, R. S. (1995) *Mol. Biol. Evol. 12*, 1063−1073.

Haas, I. G., & Wabl, M. (1983) *Nature (London) 306*, 387−389.

Harlow, E., & Lane, D. (1988) *Antibodies: A Laboratory Manual*, Cold Spring Harbor Laboratory, Cold Spring Harbor, NY.

Helenius, A. (1994) *Mol. Biol. Cell 5*, 253−265.

Iannotti, A. M., Rabideau, D. A., & Dougherty, J. J. (1988) *Arch. Biochem. Biophys. 264*, 54−60.

Jakob, U., Scheibel, T., Bose, S., Reinstein, J., & Buchner, J. (1996) *J. Biol. Chem. 271*, 10035−10041.

Janin, J., & Chothia, C. (1990) *J. Biol. Chem. 265*, 16027−16030.

Knittler, M. R., Dirks, S., & Haas, I. G. (1995) *Proc. Natl. Acad. Sci. U.S.A. 92*, 1764−1768.

Koch, G., Smith, M., Macer, D., Webster, P., & Mortara, R. (1986) *J. Cell Sci. 86*, 217−232.

Koyasu, S., Nishida, E., Kadowaki, T., Matsuzaki, F., Iida, K., Harada, F., Kasuga, M., Sakai, H., & Yahara, I. (1986) *Proc. Natl. Acad. Sci. U.S.A. 83*, 8054−8058.

Kozutsumi, Y., Segal, M., Normington, K., Gething, M.-J., & Sambrook, J. (1988) *Nature (London) 332*, 462−464.

Kuehn, M. J., Ogg, D. J., Kihlberg, J., Slonim, L. N., Flemmer, K., Berfors, T., & Hultgren, S. J. (1993) *Science 262*, 1234−1241.
Kuznetsov, G., Chen, L. B., & Nigam, S. K. (1994) *J. Biol. Chem. 269*, 22990−22995.
Lee, A. S. (1987) *Trends Biochem. Sci. 12*, 20−23.
Lenny, N., & Green, M. (1991) *J. Biol. Chem. 266*, 20532−20537.
Li, Z., & Srivastava, P. K. (1993) *EMBO J. 12*, 3143−3151.
Macer, D. R. J., & Koch, G. L. E. (1988) *J. Cell Sci. 91*, 61−70.
Mazzarella, R. A., Srinivasan, M., Haugejorden, S. M., & Green, M. (1990) *J. Biol. Chem. 265*, 1094−1101.
Melnick, J., Aviel, S., & Argon, Y. (1992) *J. Biol. Chem. 267*, 21303−21306.
Melnick, J., Dul, J. L., & Argon, Y. (1994) *Nature (London) 370*, 373−375.
Mignery, G. A., Newton, C. L., Archer, B. T., & Sudhof, T. C. (1990) *J. Biol. Chem. 265*, 12679−12685.
Minami, Y., Kawasaki, H., Yoshihiko, M., Suzuki, K., & Yahara, I. (1991) *J. Biol. Chem. 266*, 10099−10103.
Minami, Y., Kimura, Y., Kawasaki, H., Suzuki, K., & Yahara, I. (1994) *Mol. Cell. Biol. 14*, 1459−1464.
Munro, S., & Pelham, H. R. (1986) *Cell 46*, 291−300.
Nadeau, K., Das, A., & Walsh, C. T. (1993) *J. Biol. Chem. 268*, 1479−1487.
Navarro, D., Qadri, I., & Pereira, L. (1991) *Virology 184*, 253−264.
Nemoto, T., Ohara-Nemoto, Y., Ota, M., Takagi, T., & Yokoyama, K. (1995) *Eur. J. Biochem. 233*, 1−8.
Nguyen, T. H., Law, D. T. S., & Williams, D. B. (1991) *Proc. Natl. Acad. Sci. U.S.A. 88*, 1565−1569.
Nicchitta, C. V., & Blobel, G. (1993) *Cell 73*, 989−998.
Normington, K., Kohno, K., Kozutsumi, Y., Gething, M.-J., & Sambrook, J. (1989) *Cell 57*, 1223−1236.
Pelham, H. R. (1986) *Cell 46*, 959−961.
Peterson, J. R., Ora, A., Van, P. N., & Helenius, A. (1995) *Mol. Biol. Cell. 6*, 1173−1184.
Rose, M. D., Misra, L. M., & Vogel, J. P. (1989) *Cell 57*, 1211−1221.
Rothman, J. E. (1989) *Cell 59*, 591−601.
Sanders, S. L., Whitfield, K. M., Vogel, J. P., Rose, M. D., & Schekman, R. W. (1992) *Cell 69*, 353−365.
Schaiff, W. T., Hruska, K. A., Jr., McCourt, D. W., Green, M., & Schwartz, B. D. (1992) *J. Exp. Med. 176*, 657−666.
Shen, N. V., Chen, X., Boyer, M. M., & Pfaffinger, P. J. (1993) *Neuron 11*, 67−76.
Siegel, L. M., & Monty, K. J. (1966) *Biochim. Biophys. Acta 112*, 346−362.
Sorger, P. K., & Pelham, H. R. (1987) *J. Mol. Biol. 194*, 341−344.
Spence, J., & Georgopoulos, C. (1989) *J. Biol. Chem. 264*, 4398−4403.
Srivastava, P. K., DeLeo, A. B., & Old, L. J. (1986) *Proc. Natl. Acad. Sci. U.S.A. 83*, 3407−3411.
Suto, R., & Srivastava, P. K. (1995) *Science 269*, 1585−1588.
Vogel, J. P., Misra, L. M., & Rose, M. D. (1990) *J. Cell Biol. 110*, 1885−1895.
Walter, P., & Blobel, G. (1983) *Methods Enzymol. 96*, 84−93.
Wearsch, P. A., & Nicchitta, C. V. (1996) *Protein Expression Purif. 7*, 114−121.
Zhu, X., Zhao, X., Burkholder, W. F., Gragerov, A., Ogata, C. M., Gottesman, M. E., & Hendrickson, W. A. (1996) *Science 272*, 1606−1614.

BI962068Q